

Michał Bejger (INFN Ferrara)

1.7.22

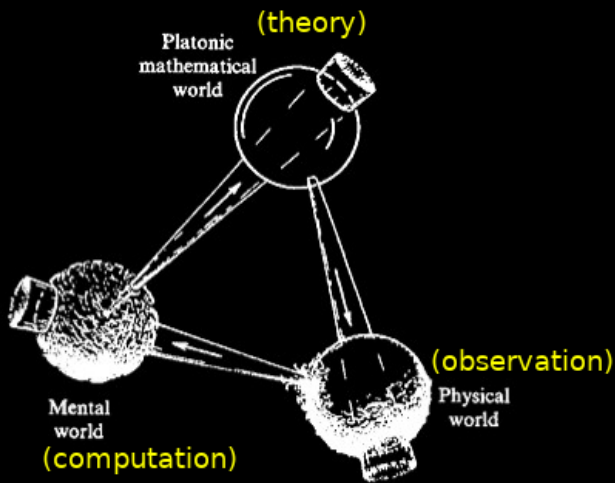


# About me: worldline

- ★ **PhD** in astrophysics (NCAC, 2005), **Marie Curie Fellowship** (Paris Observatory, 2006-2008), **habilitation** (NCAC, 2013), **DAAD scholarship** at the Steinbuch Centre for Computing (Karlsruhe, 2015), **research stay** at the APC (Paris, 2018-2019),
- ★ **Joined Virgo (LIGO-Virgo-KAGRA) in 2011**
- ★ **Interests:** dense-matter equation of state/neutron stars ★ numerical relativity ★ gravitational-wave data analysis ★ high-performance computing & machine learning.

# About me: collaboration roles

- ★ Outreach and popularization at the LIGO-Virgo-KAGRA level (2011-2020) & popular science magazine "Delta"
- ★ LIGO-Virgo-KAGRA data analysis co-chair (long-duration GWs),
- ★ Work Group leader for the G2Net COST action (ML for GW astrophysics and geophysics),
- ★ Einstein Telescope Observational Science Board division coordinator, "Scientific potentials of different detector configurations, and common tools".

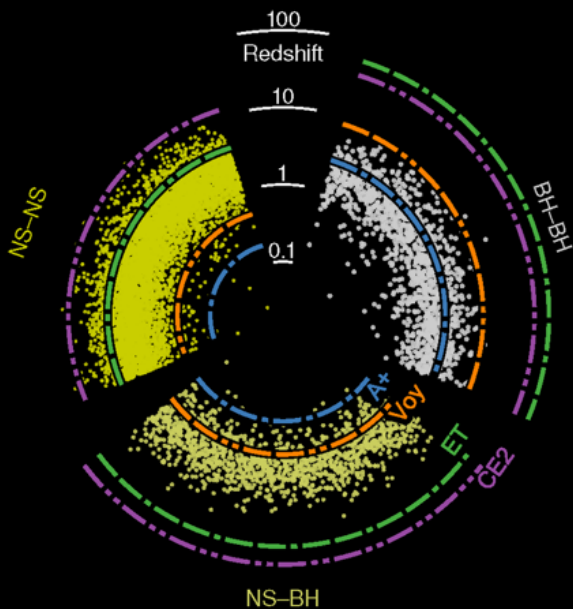


(from R. Penrose "The road to reality")

# Motivation

- ★ **theory**: NS dense matter theory, GWs,
  - ★ **observation**: GW detectors,
  - ★ **computation**: ML data analysis of GWs, numerical models of NSs.
- 
- ★ Many potential GW sources still to be discovered, e.g. long-duration CW related to NSs:
    - ★ **repeatable** studies,
    - ★ science possible in **single detector mode**,
    - **Not only NS interiors**/tests of different kinds of (astro)physics (thermal, elastic, magnetic, superfluid properties), but also
      - ★ **additional tests of GR** (polarizations etc.),
      - ★ **calibration, "distance ladder"/cosmography**,
  - ★ Machine learning/Data Analysis challenge for future detectors, to check what *is* and what *isn't* possible to establish about NSs.

# Current and future GW observations: outlook



# Recent works: arXiv:2206.13335

1. [arXiv:2206.13335](#) [pdf, other] astro-ph.HE gr-qc

## A robust argument on the existence of primordial black holes in galactic dark matter halos

**Authors:** Marek Abramowicz, Michal Bejger, Andrzej Udalski, Maciek Wielgus

**Abstract:** If primordial black holes (PBH) within the asteroid/moon-mass range indeed reside in galactic dark matter halos, they must necessarily collide with galactic neutron stars (NS). These collisions must, again necessarily, form light black holes (LBHs) with masses of typical NS,  $M_{\text{LBH}} \approx 1.5 M_{\odot}$ . LBHs may be behind events already detected by ground-based gravitational-wave detectors (GW170817, GW190425, and others such as a mixed stellar black hole-neutron star mass event GW191219\163120), and most recently by microlensing (OGLE-BLG-2011-0462). Although the status of these observations as containing LBHs is not confirmed, there is no question that gravitational-wave detectors and microlensing are in principle and in practice capable of detecting LBHs. We have calculated the creation rate of LBHs resulting from these light primordial black hole collisions with neutron stars. On this basis, we claim that if improved gravitational-wave detectors and microlensing statistics of the LBH events would indicate that the number of LBHs is significantly lower than what follows from the calculated creation rate, then this would be an unambiguous proof that there is no significant light PBH contribution to the galactic dark matter halos. Otherwise, if observed and calculated numbers of LBHs roughly agree, then the hypothesis of primordial black hole existence gets strong observational support, and in addition their collisions with neutron stars may be considered a natural creation channel for the LBHs, solving the problem of their origin, as it is known that they cannot be a product of standard stellar evolution. [△ Less](#)

Submitted 27 June, 2022; originally announced June 2022.

Comments: submitted to ApJL

# Recent works: arXiv:2206.13335

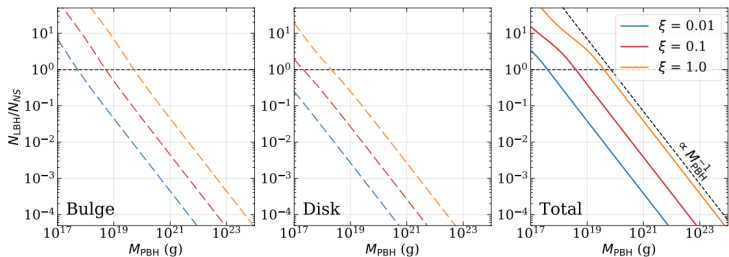


**Figure 2.** Ratio of LBH and NS densities in a model galaxy of 13 Gyears age, as a function of  $M_{\text{PBH}}$  – a characteristic mass of PBHs, for 3 different fractions of PBH in a galactic mass composition  $\xi$ . This ratio represents the expected ratio of occurrence of collisions of stellar mass BHs with LBHs and stellar mass BHs with NSs. The three panels correspond to galactic disk, bulge, and the total galaxy. For large  $\xi$  or light  $M_{\text{PBH}}$  majority of NSs may become LBHs.



# Recent works: arXiv:2205.13513

2. arXiv:2205.13513 [pdf, other] [gr-qc](#) [astro-ph.IM](#)

## Denoising gravitational-wave signals from binary black holes with dilated convolutional autoencoder

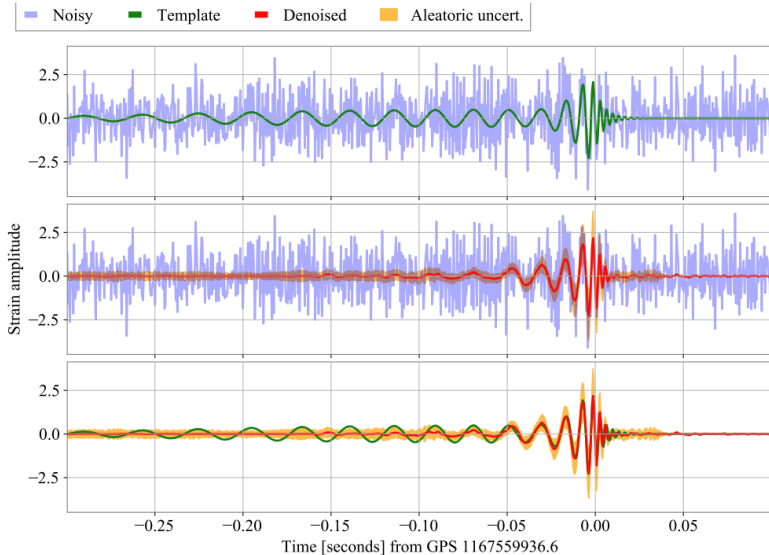
**Authors:** [P. Bacon](#), [A. Trovato](#), [M. Bejger](#)

**Abstract:** Broadband frequency output of gravitational-wave detectors is a non-stationary and non-Gaussian time series data stream dominated by noise populated by local disturbances and transient artifacts, which evolve on the same timescale as the gravitational-wave signals and may corrupt the astrophysical information. We study a denoising algorithm dedicated to expose the astrophysical signals by employing a convolutional neural network in the encoder-decoder configuration, i.e. apply the denoising procedure of coalescing binary black hole signals in the publicly available LIGO O1 time series strain data. The denoising convolutional autoencoder neural network is trained on a dataset of simulated astrophysical signals injected into the real detector's noise and a dataset of detector noise artifacts ("glitches"), and its fidelity is tested on real gravitational-wave events from O1 and O2 LIGO-Virgo observing runs. [△ Less](#)

Submitted 26 May, 2022; originally announced May 2022.

Comments: 27 pages, 5 figures in the text and 7 in the appendix

# Recent works: arXiv:2205.13513



# Recent works: arXiv:2205.02865

3. arXiv:2205.02865 [pdf, ps, other] [astro-ph.HE](#) [astro-ph.SR](#)

## Timing six energetic rotation-powered X-ray pulsars, including the fast-spinning young PSR J0058-7218 and Big Glitcher PSR J0537-6910

**Authors:** Wynn C. G. Ho, Lucien Kulper, Cristobal M. Espinoza, Sebastien Guillot, Paul S. Ray, D. A. Smith, Slavko Bogdanov, Dana Antonopoulou, Zaven Arzumanian, Michal Bejger, Teruaki Enoto, Paolo Esposito, Alice K. Harding, Brynmor Haskell, Natalia Lewandowska, Chandreyee Maitra, Georgios Vasilopoulos

**Abstract:** Measuring a pulsar's rotational evolution is crucial to understanding the nature of the pulsar. Here we provide updated timing models for the rotational evolution of six pulsars, five of which are rotation phase-connected using primarily NICER data. For the newly-discovered fast energetic young pulsar, PSR J0058-7218, we increase the baseline of its timing model from 1.4 days to 8 months and not only measure more precisely its spin-down rate  $\dot{\nu} = (-6.2324 \pm 0.0001) \times 10^{-11} \text{ Hz s}^{-1}$  but also for the first time the second time derivative of spin rate  $\ddot{\nu} = (4.2 \pm 0.2) \times 10^{-21} \text{ Hz s}^{-2}$ . For the fastest and most energetic young pulsar, PSR J0537-6910, we detect 4 more glitches, for a total of 15 glitches over 4.5 years of NICER monitoring, and show that its spin-down behavior continues to set this pulsar apart from all others, including a long-term braking index  $n = -1.234 \pm 0.009$  and interglitch braking indices that asymptote to  $\sim 7$  for long times after a glitch. For PSR J1101-6101, we measure a much more accurate spin-down rate that agrees with a previous value measured without phase-connection. For PSR J1412+7922 (also known as Calvera), we extend the baseline of its timing model from our previous 1-year model to 4.4 years, and for PSR J1849-0001, we extend the baseline from 1.5 years to 4.7 years. We also present a long-term timing model of the energetic pulsar, PSR J1813-1749, by fitting previous radio and X-ray spin frequencies from 2009-2019 and new ones measured here using 2018 NuSTAR and 2021 Chandra data. [△ Less](#)

Submitted 5 May, 2022; originally announced May 2022.

Comments: 18 pages, 17 figures; submitted to Apj

# Recent works: arXiv:2205.02865

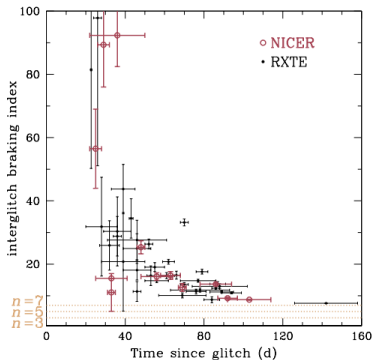


**Figure 5.** Interglitch braking index  $n_{ig}$  of PSR J0537–6910 calculated from spin parameters of each segment between glitches as a function of time since the last glitch. Large and small circles denote NICER and RXTE values, respectively (from here and Antonopoulou et al. 2018; Ho et al. 2020b; Abbott et al. 2021b). Errors in  $n_{ig}$  are  $1\sigma$ . Horizontal dotted lines indicate braking index  $n = 3, 5$ , and  $7$ , which are expected for pulsar spin-down by electromagnetic dipole radiation, gravitational wave-emitting mountain, and gravitational wave-emitting r-mode oscillation, respectively.

# Recent works: arXiv:2201.012017

10. arXiv:2201.01217 [pdf, other] astro-ph.HE gr-qc doi 10.1103/PhysRevD.105.123015

## Differentiating between sharp and smoother phase transitions in neutron stars

**Authors:** Jonas P. Pereira, Michał Bejger, J. Leszek Zdunik, Paweł Haensel

**Abstract:** The internal composition of neutron stars is still an open issue in astrophysics. Their innermost regions are impervious to light propagation and gravitational waves mostly carry global aspects of stars, meaning that only indirect inferences of their interiors could be obtained. Here we assume a hypothetical future scenario in which an equation of state softening due to a phase transition is identified and estimate the observational accuracy to differentiate a sharp phase transition from a smoother one (associated with a mixed phase/state due to the unknown value of the surface tension of dense matter) in a region of a hybrid star by means of some electromagnetic and gravitational wave observables. We show that different transition constructions lead to similar sequences of stellar configurations due to their shared thermodynamic properties. In the most optimistic case - a strong quark-hadron density jump phase transition - radius observations require fractional uncertainties smaller than 1% – 2% to differentiate mixed states from sharp phase transitions. For tidal deformabilities, relative uncertainties should be smaller than 5% – 10%. However, for masses around the onset of stable quark cores, relative tidal deformability differences associated with strong sharp phase transitions and mixed states could be much larger (up to around 20% – 30%). All the above suggests that 2.5- and 3rd generation gravitational wave detectors and near-term electromagnetic missions may be able to start assessing some particular aspects of phase transitions in neutron stars. In addition, it points to some limitations on the equation of state recovery using typical neutron star observables and the impact of systematic uncertainties on modellings of the equation of state of hybrid stars. Finally, we briefly discuss other observables that may also be relevant for the probe of mixed states in stars. [△ Less](#)

**Submitted** 23 May, 2022; **v1 submitted** 4 January, 2022; **originally announced** January 2022.

**Comments:** 17 pages, 15 figures (some updated); Improved abstract, presentation and discussions (assumptions, phase transitions, EOS recovery, predictions, etc); New references added; Accepted for publication in PRD

# Recent works: arXiv:2201.012017

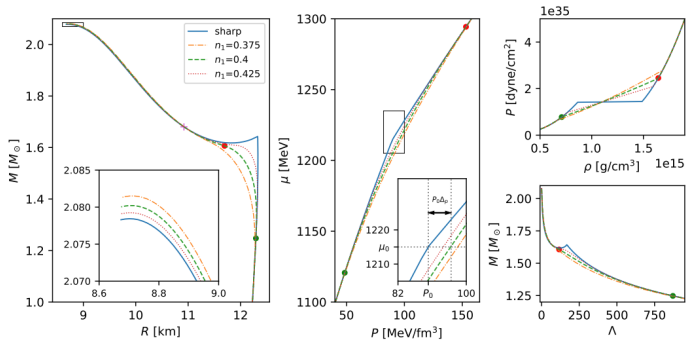


FIG. 1. Examples of polytropic EOS and resulting sequences of NS parameters (solutions of TOV equations): sharp phase transition (solid blue curves), and three mixed state realizations (dash-dotted orange curves with  $n_1=0.375 \text{ fm}^{-3}$ , dashed green curves with  $n_1=0.4 \text{ fm}^{-3}$  and dotted red curves with  $n_1=0.425 \text{ fm}^{-3}$ ). The sharp phase transition EOS parameters are  $\gamma_1 = 3.5$ ,  $\gamma_2 = 6$ , density jump (in terms of the baryon density  $n$ ) between  $n_0 = 0.475 \text{ fm}^{-3}$  and  $n_{02} = 0.76 \text{ fm}^{-3}$ . The leftmost panel contains the mass-radius  $M(R)$  sequences (the inset plot presents a closeup of the region around the maximum mass), the middle panel is the chemical potential-pressure  $\mu(P)$  relation, the upper right panel is the pressure-density  $P(\rho)$  relation, whereas the lower right one is the mass-tidal deformability  $M(\Lambda)$  relation. Green and red dots mark the beginning and the end of the mixed state region in the other panels have central parameters equal to the beginning (green dot) and the end (red dot) of the mixed state. The inset in the  $\mu(P)$  plot shows the definition of  $\Delta_p$  - marked by an arrow - on the example of the  $n_1=0.4 \text{ fm}^{-3}$  EOS, marked by the green dashed line.  $P(\mu_0)$  is denoted by  $P_0$ . Note that the for the  $M(R)$  sequences the mixed state curves are below the sharp one in the vicinity of the phase transition point, but  $M_{\text{max}}$  is larger for the mixed state EOSs. For the  $n_1=0.4 \text{ fm}^{-3}$  EOS, the mixed state and the sharp transition EOSs have the same mass and radius parameters at  $M \approx 1.68 M_\odot$  and  $\approx 10.92 \text{ km}$ , marked by a magenta cross.

# Recent works (LVK): arXiv:2201.00697

11. [arXiv:2201.00697](#) [pdf, other] [gr-qc](#) [astro-ph.HE](#)

## All-sky search for continuous gravitational waves from isolated neutron stars using Advanced LIGO and Advanced Virgo O3 data

**Authors:** The LIGO Scientific Collaboration, the Virgo Collaboration, the KAGRA Collaboration, R. Abbott, H. Abe, F. Acernese, K. Ackley, N. Adhikari, R. X. Adhikari, V. K. Adkins, V. B. Adya, C. Affeldt, D. Agarwal, M. Agathos, K. Agatsuma, N. Aggarwal, O. D. Aguiar, L. Aiello, A. Ain, P. Ajith, T. Akutsu, S. Albanesi, R. A. Alfaldi, A. Allocca, P. A. Altin, et al. (1645 additional authors not shown)

**Abstract:** We present results of an all-sky search for continuous gravitational waves which can be produced by spinning neutron stars with an asymmetry around their rotation axis, using data from the third observing run of the Advanced LIGO and Advanced Virgo detectors. Four different analysis methods are used to search in a gravitational-wave frequency band from 10 to 2048 Hz and a first frequency derivative from  $-10^{-8}$  to  $10^{-9}$  Hz/s. No statistically-significant periodic gravitational-wave signal is observed by any of the four searches. As a result, upper limits on the gravitational-wave strain amplitude  $h_0$  are calculated. The best upper limits are obtained in the frequency range of 100 to 200 Hz and they are  $\sim 1.1 \times 10^{-25}$  at 95% confidence-level. The minimum upper limit of  $1.10 \times 10^{-25}$  is achieved at a frequency 111.5 Hz. We also place constraints on the rates and abundances of nearby planetary- and asteroid-mass primordial black holes that could give rise to continuous gravitational-wave signals. [△ Less](#)

Submitted 3 January, 2022; originally announced January 2022.

Comments: 23 main text pages, 17 figures

Report number: LIGO-P2100367

# Recent works (LVK): arXiv:2201.00697

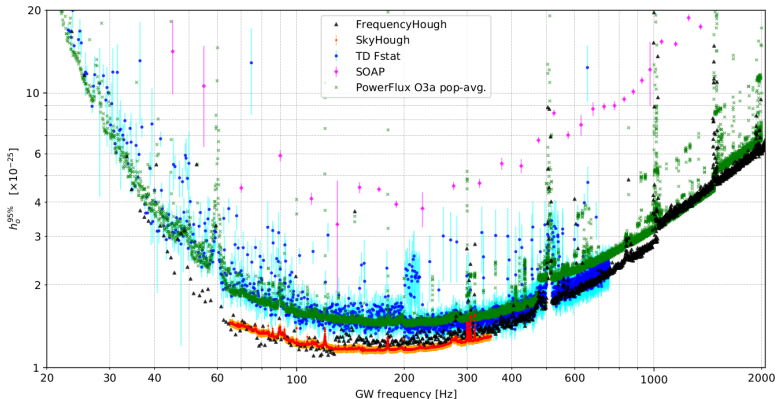


FIG. 15. Comparison of broadband search sensitivities obtained by the *FrequencyHough* pipeline (black triangles), the *SkyHough* pipeline (red squares), the *Time-Domain F-statistic* pipeline (blue circles), and the *SOAP* pipeline (magenta diamonds). Vertical bars mark errors of  $h_0$  obtained in the procedures described in Sects. IV and V. Population-averaged upper limits obtained in [102] using the O3a data are marked with dark-green crosses.